Eur Biophys J (2005) 35: 27–39
DOI 10.1007/s00249-005-0002-1

ARTICLE

**Yves-Marie Coïc · Michel Vincent · Jacques Gallay
Françoise Baleux · Florence Mousson · Veronica Beswick
Jean-Michel Neumann · Béatrice de Foresta**

# Single-spanning membrane protein insertion in membrane mimetic systems: role and localization of aromatic residues

Received: 18 January 2005 / Revised: 13 May 2005 / Accepted: 23 May 2005 / Published online: 15 July 2005


**Abstract** Membrane protein insertion in the lipid bilayer is determining for their activity and is governed by various factors such as specific sequence motifs or key amino-acids. A detailed fluorescence study of such factors is exemplified with PMP1, a small (38 residues) single-membrane span protein that regulates the plasma membrane $H^+$-ATPase in yeast and specifically interacts with phosphatidylserines. Such interactions may stabilize raft domains that have been shown to contain $H^+$-ATPase. Previous NMR studies of various fragments have focused on the critical role of interfacial residues in the PMP1 structure and intermolecular interactions. The C-terminal domain contains a terminal Phe (F38), a single Trp (W28) and a single Tyr (Y25) that may act together to anchor the protein in the membrane. In order to describe the location and dynamics of W28 and the influence of Y25 on protein insertion within membrane, we carried out a detailed steady-state and time-resolved fluorescence study of the synthetic G13-F38 fragment and its Tyr-less mutant, Y25L in various membrane mimetic systems. Detergent micelles are conveniently used for this purpose. We used dodecylphosphocholine (DPC) in order to compare with and complement previous NMR results. In addition, dodecylmaltoside (DM) was used so that we could apply our recently described new quenching method by two brominated analogs of DM (de Foresta et al. 2002, Eur. Biophys. J. 31:185–97). In both systems, and in the presence and absence of Y25, W28 was shown to be located below but close to the polar headgroup region, as shown by its maximum emission wavelengths ($\lambda_{max}$), curves for the quenching of Trp by the brominated analogs of DM and bimolecular constants for quenching ($k_q$) by acrylamide. Results were interpreted by comparison with calibration data obtained with fluorescent model peptides. Time-resolved anisotropy measurements were consistent with PMP1 fragment immobilization within peptide-detergent complexes. We tentatively assigned the two major Trp lifetimes to the Trp ($\chi_1 = 60°$ and 180°) rotamers, based on the recent lifetime–rotamer correlation proposed for model cyclic peptides (Pan and Barkley 2004, Biophys J 86:3828–35). We also analyzed the role of the hydrophobic anchor, by comparing the micelle binding of fragments of various lengths including the synthesized full-length protein and detected peculiar differences for protein interaction with the polar headgroups of DM or DPC.

**Keywords** PMP1 fragments · Aromatic interfacial residues · Steady-state and time-resolved fluorescence · Brominated detergents · Dodecylmaltoside and dodecylphosphocholine micelles

**Abbreviations** PMP1 (or 2): Plasma membrane proteolipid 1 (or 2) · PLN: Phospholamban · SLN:

Y.-M. Coïc · F. Baleux
Unité de Chimie Organique, Institut Pasteur,
URA CNRS 487, 28 rue du Dr. Roux,
75724 Paris Cedex, France

M. Vincent · J. Gallay
Laboratoire pour l'Utilisation du Rayonnement
Electromagnétique, Université Paris-Sud,
UMR CNRS 130, Orsay, France

F. Mousson · V. Beswick · J.-M. Neumann · B. de Foresta (✉)
Service de Biophysique des Fonctions Membranaires,
Centre d'Etudes de Saclay, CEA DSV/DBJC
and URA CNRS 2096, 91191
Gif sur Yvette Cedex, France
E-mail: foresta@dsvidf.cea.fr
Tel.: +33-1-69088944
Fax: +33-1-69088139

*Present address*: M. Vincent · J. Gallay
Centre Universitaire Paris-Sud,
UMR CNRS 8619, Bât. 430,
91405 Orsay Cedex, France

*Present address*: V. Beswick
Université d'Evry, Bd F. Mitterrand,
91025 Evry, France

*Present address*: F. Mousson
Laboratory for Physiological Chemistry,
University Medical Centre-Utrecht,
3508 AB Utrecht, The Netherlands

Sarcolipin · DM: Dodecylmaltoside · BrDM: 7,8-dibromododecylmaltoside · BrUM: 10,11-dibromoundecanoylmaltoside · DPC: Dodecylphosphocholine · SDS: Sodium dodecyl sulfate · POPS: 1-palmitoyl-2-oleoyl-3-glycerophosphatidylserine · NATA: *N*-acetyltryptophanamide · TOE: Tryptophan octyl ester · SR: Sarcoplasmic reticulum · MEM: Maximum entropy method · P3: $K_2WL_9AL_9K_2A$ · P5: $K_2CLWL_7AL_9K_2A$ · P7: $K_2CL_3WL_5AL_9K_2A$ · P9: $K_2CL_5WL_3AL_9K_2A$ · P11: $K_2CL_7WLAL_9K_2A$ · P13: $K_2CL_9WL_9K_2A$ · HATU: *O*-(7-azabenzotriazol-1-yl)-1,1,3,3-tetramethyluronium hexafluorophosphate · DIPEA: *N,N*-diisopropylethylamine · TFA: Trifluoroacetic acid · MPLC: Medium-pressure liquid chromatography

## Introduction

PMP1 and PMP2 are small (38 amino acids) single membrane-span proteins that have been shown to regulate the plasma membrane $H^+$-ATPase in yeast (Navarre et al. 1994; Navarre et al. 1992). They differ by only one amino acid (A21 or S21) and are structurally and functionally similar to known regulatory proteolipids, such as phospholamban (PLN), sarcolipin (SLN)—regulating the cardiac and skeletal muscle $Ca^{2+}$-ATPases, respectively—and the $\gamma$-subunit of the mammalian $Na^+$ -$K^+$-ATPase. These small proteolipids (31 to 58 amino-acids) all share a single transmembrane α-helix located at the N-terminal end (PMP1, see sequence below), in the center (SLN, $\gamma$-subunit) or at the C-term (PLN) of the protein. This transmembrane segment may act both as a membrane anchor and as an interaction domain with ATPase transmembrane helices (presumably with the transmembrane helices 4 and 6 of $Ca^{2+}$-ATPase in the case of SLN and PLN) (Asahi et al. 1999; Asahi et al. 2003; Beswick et al. 1998b ; Jones et al. 2001; Mascioni et al. 2002; Zamoon et al. 2003). Synthetic PMP1 fragments have also been shown to sequester a subset of negatively charged phospholipids, POPS, a prominent component of the inner leaflet of the yeast plasma membrane. Previous NMR studies have focused on the structural properties of these fragments and described in detail such POPS–PMP1 interactions (Beswick et al. 1998a,b; Mousson et al. 2001a,b, 2002; Roux et al. 2000), which may be related to the occurrence of raft domains.

The sequence of PMP1 is $L_1$-P-G-G-$V_5$-I-L-V-F-$I_{10}$-L-V-G-L-$A_{15}$-C-I-A-I-$I_{20}$- **A-T-I-I-$Y_{25}$-R-K-W-Q-$A_{30}$-R-Q-R-G-$L_{35}$-Q-R-$F_{38}$**. This protein comprises an N-terminal membrane-spanning domain and a C-terminal positively charged cytoplasmic domain (in bold). The A18-F38 fragment (Beswick et al. 1998a, b; Roux et al. 2000) and particularly the G13-F38 fragment (Mousson et al. 2001a, 2002), which encompasses a significant part of the membrane-spanning domain and the entire C-terminal domain, are well-suited for use in detailed studies of the cytoplasmic interface. These fragments have been shown to retain the main structural elements identified in F9-F38, the longest fragment studied to date (Mousson et al. 2001b). $^1$H NMR experiments for all the fragments indicate the formation of a single transmembrane helix extending from the N-terminus to Q32 (Beswick et al. 1998b; Mousson et al. 2001a, b). The R33-F38 residues immediately following this helix form a loop that folds back towards the inside of the membrane, thereby burying the terminal phenylalanine aromatic ring in the membrane (see the working model in Beswick et al. 1998b). G13-F38 (like PMP1) contains a single (W28) Trp residue, making it possible to carry out detailed fluorescence characterization of its location and dynamics. A single Tyr (Y25) residue is also present about one helix turn before the Trp residue. The interfacial domains of membrane proteins have been shown to be enriched in both Tyr and Trp residues that are thought to be involved in the precise anchorage of membrane-spanning domains (de Planque et al. 2003; Ridder et al. 2000; Ulmschneider and Sansom 2001). W28 has been shown to be one of the critical residues of PMP1, because the W28L mutant of G13-F38 displays nonnative elements such as propagation of the α-helix up to L35 instead of Q32 (Mousson et al. 2001a).

We report here a detailed fluorescence study of G13-F38 and the Y25L mutant peptide in membrane mimetic systems composed of DM or DPC detergent micelles. Such media have already been shown to mimic quite faithfully protein or peptide embedding into the membrane (e.g., Møller et al. 1986; le Maire et al. 2000; Fernández and Wüthrich 2003, for a recent review based on NMR experiments). We chose DM because this detergent has proved to be suitable for the solubilization, the maintenance of activity and the crystallization of a wide range of membrane proteins. We also recently developed an original method for evaluating Trp depth by quenching this residue in mixed micelles of DM and two of its brominated analogs, 7,8-dibromododecylmaltoside (BrDM) and 10,11-dibromoundecanoylmaltoside (BrUM), and comparing the results with calibration data obtained with a set of fluorescent model peptides (de Foresta et al. 2002 and references cited therein). We also chose DPC because it generates an interfacial region very similar to that generated by phospholipids and that its small micelles facilitate structural measurements by NMR (Beswick et al. 1998a; Lauterwein et al. 1979). We could therefore complement and make comparison with the previous NMR studies. Note also that the structure of Y25L in this detergent is roughly close to that of the native fragment, with a unique N-terminal helix, which might be slightly extended (Mousson et al. 2001a).

The microenvironment surrounding Trp residues (particularly polarity) is known to affect their fluorescence emission (Lakowicz 1999; Reshetnyak et al. 2001; Vivian and Callis 2001). This makes it possible to follow peptide-detergent interaction and to evaluate peptide

insertion within peptide-detergent complexes. We analyzed the location of Trp in DM in more detail, using quenching by brominated DM analogs. We also determined the accessibility of Trp to acrylamide, a water-soluble quencher, in both DM and DPC. Time-resolved fluorescence intensity provided us with the distribution of Trp lifetimes, interpreted in terms of the distribution of Trp rotamers. Anisotropy decays provided rotational correlation times for Trp within the peptide-detergent complexes. This analysis should detect any static or dynamic differences between the two mutants. Binding experiments were also performed to analyze the role of the hydrophobic anchor in membrane interaction. For these experiments, we used the whole PMP1 protein-the synthesis of which was realized for the first time- and the three fragments, Y25-F38, G13-F38 and its mutant Y25L.

## Materials and methods

### Solutions and chemicals

DM was obtained from Calbiochem. Its brominated derivatives, 7,8-dibromododecylmaltoside (BrDM) and 10,11-dibromoundecanoylmaltoside (BrUM) were synthesized as previously described (de Foresta et al. 1999; de Foresta et al. 1996). DPC was obtained from Avanti Polar Lipids (AL, USA). *N*-acetyltryptophanamide (NATA) and acrylamide were purchased from Sigma-Aldrich. Methanol and ethanol were obtained from Merck (Uvasol quality). Stock solutions of the detergents were prepared in water at concentrations of 20 and 200 mM. The stock solution of acrylamide was 5 M in water. The water used was purified with a Milli-Q system. Buffers were filtered through Millex-HA filters (0.45 μM pore size; Millipore).

### Peptides

The PMP1 fragment G13-F38 (M = 3072), the mutated version of this peptide (Y25L) (M = 3022) and the shorter fragment Y25-F38 (M = 1934) were synthesized as previously described (Mousson et al. 2001a, b). The Cys16 residue in the first two fragments was replaced with a serine and all the peptides were acetylated at the N-terminus and amidated at the C-terminus. All fragment preparations were over 99% pure. Stock solutions (1 mM) (kept at 4°C, protected from light) were prepared in methanol, in which the peptides were readily soluble.

The entire PMP1 peptide was synthesized by means of a solid-phase Fmoc chemistry protocol (Chan and White 2000), on a Pioneer continuous-flow peptide synthesizer (Applied Biosystems, Foster City, CA, USA). Extended double-coupling cycles were performed with a four-fold molar excess of Fmoc-amino acid derivatives, with HATU and DIPEA as coupling reagents. A Fmoc-L-Phe-PEG-PS support was used, resulting in a free carboxyl terminus. All chemical reagents were purchased from Applied Biosystems. Cleavage was obtained by incubation with 84% TFA, 6% phenol, 4% water, 2% triisopropylsilane, 2% thioanisol, 2% ethanedithiol for 3 h at room temperature. The cleavage products were removed from the resin and deprotected. They were then precipitated in cold diethyl ether, filtered, dissolved in aqueous TFA buffer and lyophilized. Crude peptide was dissolved in 0.08% aqueous TFA/acetonitrile and was directly purified by reverse-phase MPLC, using a Nucleoprep 20 μm C4 100 Å preparative column and a 60-min linear gradient (1.2%/min) of acetonitrile: 2-propanol (7:3, v/v) in 0.08% aqueous TFA (pH 2) at a flow rate of 18 ml/min. In these conditions, PMP1 was eluted at a very high concentration (82%) of organic phase.

An additional step of purification by RP-HPLC was required, on a nucleosil 5 μm C4 300 Å semi-preparative column, using the same eluents with a 2%/min linear gradient over 20 min, with a flow rate of 6 ml/min. We checked the purity of the peptides by HPLC on a nucleosil 5 μm C4 300 Å analytical column, using a similar gradient, and a flow rate of 1 ml/min. The purified peptide (total yield 1.7%) was characterized by positive ion electrospray ionization mass spectrometry (experimental data 4251.95 ± 0.35—expected mass 4252.25). Stock solutions (1 mM) were also prepared in methanol.

### Absorption measurements

Absorption spectra were recorded on an HP8453 diode array spectrophotometer, with a thermostatically controlled sample holder (20°C). The sample was continuously stirred. The pathlength through the cuvette was 1 cm.

### Steady-state fluorescence measurements

Fluorescence data were obtained on a Spex Fluorolog spectrofluorometer. The temperature in the cuvette was controlled with a thermostat and the sample was continuously stirred. We used a standard quartz cuvette (1×1 cm). Excitation spectra were corrected for the spectrum of the lamp and both excitation and emission spectra were corrected for fluctuations in light intensity (usually very small, < 1%). Fluorescence maxima $\lambda_{max}$ were reproducible within ± (0.5–1 nm). Slit widths were usually of 1.25 mm (bandwidths ~5 nm) unless otherwise stated.

### Time-resolved fluorescence measurements

Fluorescence intensity and anisotropy decays were determined by the time-correlated single photon counting technique from the polarized components, $I_{vv}(t)$ and $I_{vh}(t)$, on the experimental setup of the SB1 window of the synchrotron radiation machine Super-ACO (Anneau

de Collision d'Orsay), as previously described (Rouvière et al. 1997 and references cited therein). The excitation and emission wavelengths were selected with a double (Jobin Yvon UV-DH10) and a single monochromator (Jobin Yvon UV-H10), respectively. A Hamamatsu MCP-PMT (model R3809U-02) was used as the detector. The time resolution was about 20 ps and the data were accumulated in 2,048 channels. Automatic sampling cycles were carried out, including 30 s accumulation time for the instrument response function and 90 s acquisition time for each polarized component, so that a total of (2–4)×$10^6$ counts was reached for each fluorescence intensity decay. Fluorescence intensity and anisotropy decays—$I(t)$ and $A(t)$, respectively—were analyzed as sums of 150 exponential terms by the maximum entropy method (MEM) (Livesey and Brochon 1987) according tothe following equations:

$$I(t) = \sum_i \alpha_i \exp(-t/\tau_i)$$

where $\alpha_i$ is the normalized amplitude and $\tau_i$ the lifetime of the intensity decay, and

$$A(t) = \sum_i \beta_i \exp(-t/\theta_i)$$

where $\beta_i$ is the anisotropy and $\theta_i$ the rotational correlation time of the anisotropy decay. In this second analysis, we assume that each lifetime $\tau_i$ is associated with all rotational correlation times $\theta_i$.

MEM does not impose any particular number of significant parameters of the decay. To ensure that the recovered distribution agrees with the data, the Skilling–Jaynes entropy S is subjected to a $\chi^2$ constraint (Brochon 1994).

## Calculation of the micelle theoretical rotational correlation time

Assuming that $\theta = \eta V/RT$, where $V$ is the spherical volume of the rotor ($V = M_w v$, $M_w$ being the molecular weight of the rotor, i.e., the micelle, and $v$ its partial specific volume) and $\eta$ the viscosity of the medium (with $\eta = 1$ cP for water at 20°C), a value of $\theta = 21$ ns was calculated for DM micelles [with $M_w =$ nM, with $M$, the molecular weight of DM being 511 and n the aggregation number of the micelles taken as $n = 125$ (±10%), mean value from Møller and le Maire (1993) and Dupuy et al. (1997) and $v = 0.81$ $cm^3/g$ (Peterson et al. 1988)]. For DPC micelles, we obtained $\theta = 7.4$ ns [with M = 352, $n = 55$ (±10%) and $v = 0.937$ $cm^3/g$ (Brown et al. 1981; Lauterwein et al. 1979)]. Experimental values might be slightly higher due to micelle hydration and asymmetry.

## Analysis of the fluorescence quenching data

Quenching by acrylamide was analyzed using the classical Stern-Volmer equation (see, for reviews, Eftink (1991); Lakowicz (1999)):

$$F_0/F = 1 + K_{sv}[Q]$$

where $K_{sv}$ is the Stern-Volmer quenching constant and [Q] is the quencher concentration. $K_{sv}$ is related to the bimolecular quenching constant $k_q$ by the following formula:

$$K_{sv} = k_q \tau_0$$

where $\tau_0$ is the lifetime, in the absence of quencher, of the fluorophore.

We analyzed fluorescence quenching by brominated detergents in mixed micelles of DM with a brominated analog by means of the quenching model first described by London and Feigenson (1981) and used by East and Lee (1982): this model was originally designed to describe the quenching of membrane fluorophores (e.g. protein Trp) by spin-labeled or brominated phospholipids. This model considers two populations of fluorophores: one completely inaccessible to the quencher and responsible for the residual fluorescence $F_{min}$ (e.g. Trp embedded in a protein), and one in which each fluorophore has $n$ neighbors (phospholipids) and for which fluorescence is completely quenched if one (or more) of these sites is occupied by a modified phospholipid. Phospholipids are supposed not to exchange their positions during the lifetime of the fluorophore. If $X$ is the molar fraction of quenchers in the membrane, then $(1\text{-}X)^n$ is the probability that none of the $n$ sites is occupied by a quencher. The fluorescence ratio is therefore given by: $F/F_0 = (1\text{-}F_{min}/F_0)(1\text{-}X)^n + F_{min}/F_0$. We previously applied this model to the quenching of a model compound for Trp, tryptophan octyl ester (TOE), and of transmembrane model peptides by a brominated detergent in a micellar system (de Foresta et al. 1999, 2002). Due to dynamic quenching (occurring in addition to static quenching), as shown by Trp lifetime measurements, and to the lateral and transverse inaccessibility of Trp, $n$ is not expected to give an exact determination of quenchers around Trp. It is, however, correlated to the accessibility of this residue to brominated alkyl chains. Using a set of six model peptides with Trp at various positions in the sequence (positions 3, 5, 7, 9 and 13 of 25 amino-acid polyLeu-type peptides), we established calibration curves for the parameter $n$ (de Foresta et al. 2002). We used these data as reference to which the results obtained were compared.

## NMR experiments

A 2 mg of Y25-F38 was dissolved in 500 µl of 90:10 $H_2O$:$D_2O$ sodium phosphate buffer (20 mM, pH 5) in the absence and presence of 50 mg DM. $^1H$ NMR experiments were carried out on a DRX 500 Bruker spectrometer at 35°C as previously described (Mousson et al. 2001b).

## Results

### Steady-state fluorescence spectra for the G13-F38 and Y25L peptide fragments in various media

Figure 1a shows the fluorescence spectra for G13-F38 and the mutated peptide Y25L in methanol, a medium in which these peptides were readily soluble and which was used as a reference. Y25L (which contains a single Trp and no Tyr) displayed an excitation spectrum characteristic of Trp with a maximum (at ~277 nm) and a shoulder (close to 290 nm). The wavelength at which emission was maximal ($\lambda_{max}$) was 338 nm, similar to that for the model peptides P3-P13 in the same medium (337 ± 1 nm) (de Foresta et al. 2002) indicating the presence of a Trp exposed to methanol. For G13-F38 (a single Trp and a single Tyr), the Tyr residue made only a very small and indirect contribution to fluorescence. This contribution is revealed by the slightly different shape of the excitation spectrum from that for Y25L. However, the maximum intensities of the excitation and emission spectra were only slightly greater than for Y25L (not shown). and the normalized emission spectra of G13-F38 and Y25L could almost be superimposed. This is consistent with a (Förster) Tyr–Trp transfer (Tyr and Trp are located in positions $n$ and $n+3$ of the sequence and the characteristic Förster distance for Tyr–Trp transfers is in the range of 10–15 Å). In addition, the normalized emission spectra for G13-F38 could be superimposed if the excitation wavelength was set at 280 nm or 295 nm (a wavelength at which Tyr absorption is negligible; not shown).

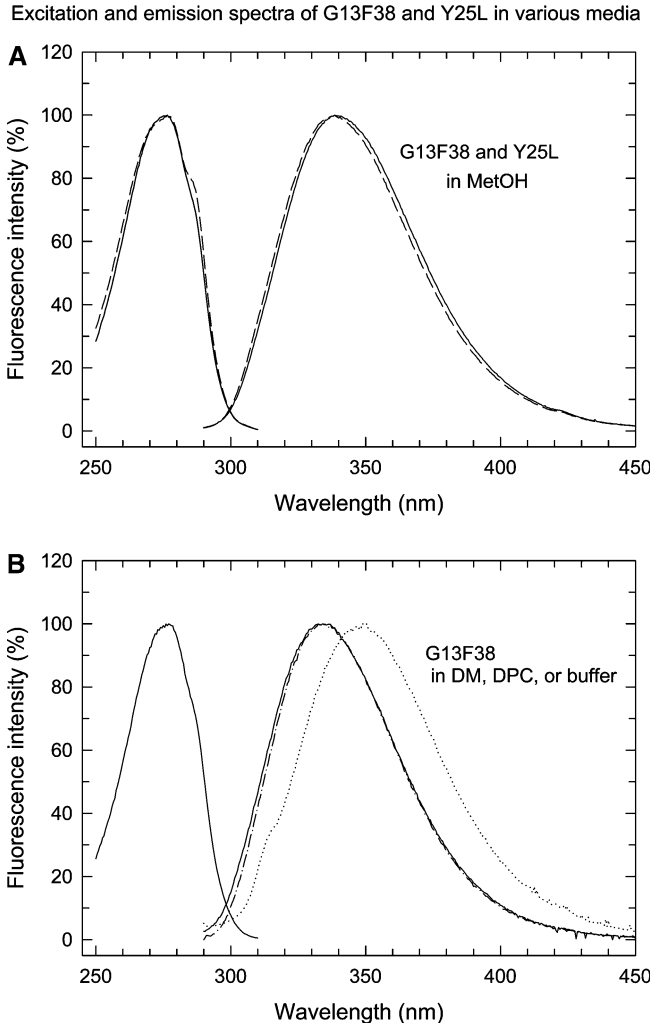


**Fig. 1** Fluorescence excitation and emission spectra of G13-F38 and its mutated form, Y25L, in various media. **a** Normalized excitation (*left*) and emission (*right*) spectra of G13-F38 (*continuous line*) and Y25L (*dashed line*; both at a concentration of 10 μM) in methanol, at 20°C. For the excitation spectra, $\lambda_{em}$was set at 339 nm (~$\lambda_{max}$) and for the emission spectra, $\lambda_{ex}$ was set at 280 nm. Before normalization, relative maximum emission intensities were one for G13-F38 and ~0.84 for Y25L. **b** Normalized excitation (left) spectrum of G13-F38 (5 μM) in the presence of 4 mM DM (in 10 mM potassium phosphate buffer, pH 7.5) (*continuous line*) and emission spectra (*right*) in 4 mM DM (*continuous line*), 4 mM DPC (*dash-dot line*) or buffer (*dotted line*), at 20°C. For the excitation spectrum, $\lambda_{em}$ was set at 334 nm and for the emission spectra, $\lambda_{ex}$ was set at 280 nm. Before normalization, relative maximum emission intensities were one in DM, 0.93 in DPC and 0.66 in buffer

Figure 1b shows the fluorescence spectra obtained for G13-F38 in the presence of an excess of detergent micelles and in aqueous buffer (10 mM potassium phosphate buffer, pH 7.5, 20°C). The excitation spectrum of G13-F38 in the presence of DM micelles resembles that obtained in methanol. The normalized emission spectra of G13-F38 in DM and DPC resemble each other but are shifted towards shorter wavelengths than the spectra obtained in methanol ($\lambda_{max}$ = 334 nm versus 338 nm) or in buffer (see below). This indicates that G13-F38 interacts with both detergents, resulting in a Trp environment, in the peptide-detergent complexes, less polar than methanol. The $\lambda_{max}$ obtained in DM and DPC is, however, slightly greater than that observed for the model peptides P3, P5 and P7 embedded within DM (325–327 nm) (de Foresta et al. 2002) or DPC (327–330 nm) (de Foresta et al., unpublished results) micelles. G13-F38 is also readily soluble in buffer alone at the concentrations tested (μM range), with a $\lambda_{max}$ (349 nm) similar to that observed when Trp is completely accessible to the aqueous medium (in NATA, for example, for which $\lambda_{max}$ ~352 nm when measured on the same apparatus (de Foresta et al. 1999)). Similar emission spectra (± 1 nm) were obtained for Y25L in the same conditions (not shown) suggesting that the environment of Trp was similar to that for G13-F38, at least in terms of polarity.

The observed solubility of these peptides in buffer led us to investigate their binding to detergent micelles.

### Curves for the binding of G13-F38, the mutated form of this peptide (Y25L), Y25-F38 and L1-F38 to detergent micelles

We investigated the binding of G13-F38 and Y25L to DM and DPC micelles (Fig. 2). This binding results in

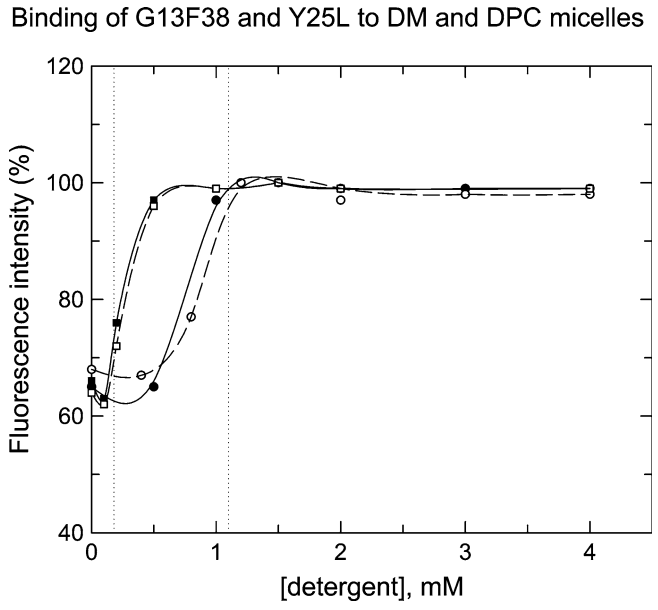


**Fig. 2** Binding of G13-F38 and its mutated form Y25L to DM (squares) or DPC (circles) micelles. G13-F38 (closed symbols) or Y25L (open symbols) (8 μM) was added to 10 mM phosphate buffer, pH 7.5, at 20°C, and fluorescence intensity recorded for 100 s to check for stabilization. Aliquots of DM (squares) or DPC (circles) were then added sequentially, with continuous stirring, at 100 s intervals. Fluorescence intensity was recorded continuously with $\lambda_{ex}$ and $\lambda_{em}$ set at 280 and 334 nm, respectively, and bandwidths of 1.25 mm (~5 nm) for both excitation and emission. The fluorescence intensities obtained after each addition of detergent, corrected for the low values obtained for the blank (detergent in buffer), were plotted as a % of the maximal value, as a function of total detergent concentration. Detergent cmcs are indicated as dotted lines

both a shift towards shorter wavelengths of the fluorescence spectrum (blue-shift) and an increase in maximum fluorescence intensity due to a decrease in polarity of the environment surrounding the Trp residue. We studied binding by monitoring increases in fluorescence intensity at 334 nm (i.e., the $\lambda_{max}$ of the spectrum at maximal detergent concentration, 4 mM).

Although the peptides were readily soluble in aqueous medium, recording the time course of fluorescence intensity showed that changes were immediate upon detergent addition as soon as interaction occurred, i.e., in the range of each detergent critical micelle concentration (cmc) (~0.18 and 1.1 mM for DM and DPC, respectively; see vertical dotted lines in Fig.2) (kinetics not shown).

G13-F38 and Y25L did not differ significantly in binding to a given detergent. As for the comparison between DM and DPC, in both cases, interaction was respectively detected close to and slightly below (for DPC) detergent cmc and binding was achieved in a narrow range of detergent concentrations (e.g., 0.2–0.5 mM for DM). This suggests that, at low detergent concentrations at least, several peptides may be present in a single micelle, becoming dispersed between different micelles with increasing detergent concentration. The shift between the curves obtained with DM or DPC was slightly smaller than the differences in cmc for these two detergents, which may indicate a slightly more favorable interaction with DPC and possible binding of monomeric DPC to peptides, preceding their insertion into micelles. These curves well illustrate the amphipathic character of these peptides, which are readily soluble in buffer but also display a strong affinity for detergent micelles.

For comparison, we investigated the interaction of the whole PMP1 protein (i.e., L1-F38) and of the shorter fragment Y25-F38 (the charged C-terminal domain, which lacks the anchor) with DM and DPC micelles, based on fluorescence intensity measurements at constant wavelength (Fig. 3). Y25-F38 bound to micellar DPC only gradually because fluorescence intensity continued to increase up to 8 mM DPC (a 1000-fold molar excess of detergent over peptide). Binding was also correlated with a blue-shift in the emission spectrum, with $\lambda_{max}$ varying from ~348 nm (Trp accessible to the aqueous buffer) to 335 nm or slightly below (not shown). Therefore, when Y25-F38 is bound, the environment of W28 is similar to that in G13-F38 fragments. These results are consistent with the transition from a highly disordered state of Y25-F38 in buffer to a well-defined conformation in the presence of DPC, allowing interaction with the micelle, as shown from $^{1}$H-NMR experiments (Mousson et al. 2001b). The peptide prob-

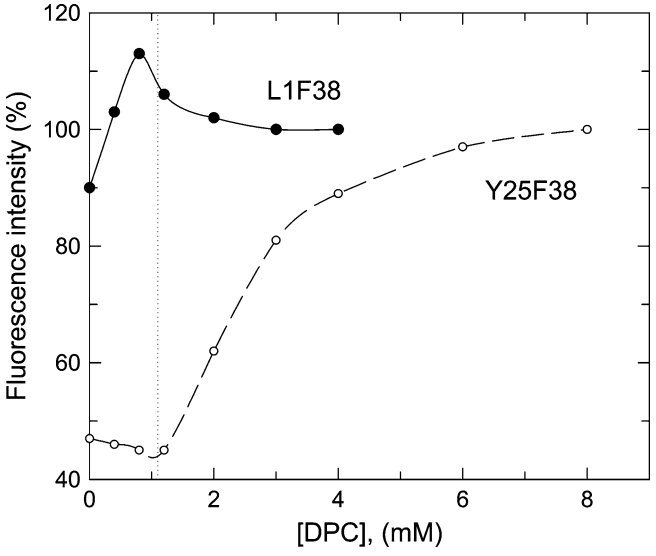


**Fig. 3** Interaction of L1-F38 and Y25-F38 with DPC. L1-F38 (closed circles) or Y25-F38 (open circles) (~8 μM) was added to 10 mM phosphate buffer, pH 7.5, at 20°C, and fluorescence recorded for 250 s to check for stabilization. Aliquots of DPC were then added sequentially, with continuous stirring, at 100 s intervals. Fluorescence intensity was recorded continuously, with $\lambda_{ex}$ and $\lambda_{em}$ set at 280 and 335 nm, respectively, and bandwidths of 1.25 mm (~5 nm) for both excitation and emission. The fluorescence intensities obtained after each addition of detergent, corrected for the low values obtained with the blank (detergent in buffer), were plotted as a % of the values obtained at maximal detergent concentration. Dotted vertical line: DPC cmc

ably lies parallel to the aqueous/detergent interface, with both N-term (with Y25 and W28) and C-term (with F38) aromatic residues more deeply embedded in the micelle. In contrast, Y25-F38 did not seem to bind to DM, as shown by the absence of significant changes in fluorescence intensity. No significant change in $\lambda_{max}$ was observed either. The absence of interaction was also checked by $^{1}$H NMR. We did not observe any significant peak shifts or line broadening in the low field region of the $^{1}$H-NMR spectrum for Y25-F38 in DM when compared to buffer (not shown). Therefore, DM does not seem to provide the interactions sufficient for the structuring of this peptide, which is required even for partial insertion in the micelle.

A biphasic curve was obtained for the more hydrophobic peptide, L1-F38, in DPC: a slight increase in fluorescence at concentrations below the cmc for DPC may result from the binding of monomeric detergent to hydrophobic patches of L1-F38 or to peptide aggregates, the presence of which is suggested by the $\lambda_{max}$ of ~335 nm. Above the cmc, fluorescence intensity decreased slightly, suggesting that the insertion of L1-F38 into detergent micelles caused only a slight change in the polarity of the environment of Trp as this residue was already in an environment of low polarity. The observed stabilization of the fluorescence signal (not shown) is also consistent with this interpretation. The interaction of L1-F38 with monomeric or micellar DM also implies the existence of various steps and involves gradual binding of L1-F38 to micellar DM, as small changes in fluorescence continued to be observed well above the cmc for DM (not shown).

These data illustrate the various peptide-detergent interactions, depending on the length of the hydrophobic anchor of the fragments and the nature of the interface between the detergent and the aqueous medium.

## Time-resolved fluorescence measurements for G13-F38 and Y25L in detergent micelles and buffer

Table 1 shows the parameters of the fluorescence intensity decays. In buffer, a classic lifetime distribution was observed for G13-F38 and Y25L, with three lifetime components (~0.5, 2.8 and 5.3 ns), with identical parameters for both fragments.

G13-F38 and Y25L lifetime distributions in DPC micelles are shown in Fig. 4. These distributions were very similar (see parameters in Table 1), but an additional minor short-lived component was observed in the distribution when compared to results in buffer (100–150 ps). Two intermediate components, centered at ~0.5 and ~3 ns, accounted for ~70% of the total amplitude. The parameters in DM differed only slightly from those in DPC and very similar results were obtained for both fragments, indicating that the Y25 mutation induced no significant change. The lifetime distributions of PMP1 fragments in detergent were strikingly different from those observed for the single Trp residue in transmembrane model peptide incorporated either in DM (de Foresta et al. 2002) or in DPC (de Foresta et al. unpublished results). In particular, they showed a much smaller proportion of long lifetime. According to the rotamer model for lifetime interpretation (e.g. Pan and Barkley 2004; Ross et al. 1992; Szabo and Rayner 1980; Willis et al. 1994), these differences should mainly reflect changes in the distribution of Trp rotamers and therefore reveal differences in conformation. The lifetime distribution of the model peptides with Trp at various positions, which exhibited a significant proportion of the longest lifetime, agreed with a significant content of α-helix (Willis et al. 1994; Bouhss et al. 1996). The different distribution for PMP1 peptides should reflect a specific folding as shown by NMR (Mousson et al. 2001a). DM also allows the formation of this specific structure. In both detergents, the minor short-lived component, corresponding to the most quenched component, may result from the proximity of W28 and the polar groups of Q32.

Mean lifetime $<\tau>$ for the two fragments was slightly longer in DM than in DPC (2.3 ns versus 1.8 ns). Similar $<\tau>$ values in DM (de Foresta et al. 2002) or in DPC (de Foresta et al., unpublished results) were only obtained for P7 to P13, whereas P3 and P5 exhibited significantly higher values (from ~4.5 to 3 ns).

The parameters of the anisotropy decays of the two fragments are given in Table 2. In buffer, anisotropy decays were characterized by two short rotational cor-

**Table 1** Parameters of the fluorescence intensity decays of G13-F38 and Y25L in DPC or DM micelles, or buffer

| Peptide | Solvent | $\alpha_1$ | $\alpha_2$ | $\alpha_3$ | $\alpha_4$ | $\tau_1$ (ns) | $\tau_2$ (ns) | $\tau_3$ (ns) | $\tau_4$ (ns) | $<\tau>$ (ns) | $\chi^2$ |
|---|---|---|---|---|---|---|---|---|---|---|---|
| G13-F38 | DPC | 0.15 | 0.35 | 0.45 | 0.05 | 0.11 | 0.49 | 3.02 | 7.36 | 1.91 | 0.95 |
| Y25L | | 0.30 | 0.25 | 0.36 | 0.09 | 0.15 | 0.47 | 2.78 | 6.20 | 1.72 | 1.05 |
| G13-F38 | DM | 0.10 | 0.36 | 0.41 | 0.13 | 0.10 | 0.47 | 3.12 | 6.02 | 2.26 | 1.06 |
| Y25L | | 0.16 | 0.31 | 0.45 | 0.09 | 0.15 | 0.60 | 3.30 | 6.95 | 2.31 | 0.97 |
| G13-F38 | Buffer | | 0.31 | 0.58 | 0.11 | | 0.57 | 2.74 | 5.07 | 2.34 | 1.03 |
| Y25L | | | 0.31 | 0.58 | 0.10 | | 0.53 | 2.83 | 5.54 | 2.38 | 0.98 |

Peptides were dissolved in 10 mM potassium phosphate buffer pH 7.5 supplemented with 4 mM DPC or DM, at a concentration of 5 μM, or in buffer, at a concentration of 10 μM, at 20°C. $\lambda_{ex}$ = 292 nm (to minimize possible Tyr to Trp fluorescence transfers), $\lambda_{em}$ = 334 nm in the presence of detergent, and 350 nm in buffer (slit widths: 4 and 8 nm for excitation and emission, respectively). $\alpha_i$ is the normalized area and $\tau_i$ the barycenter of each peak of the lifetime distribution, obtained by MEM analysis. The mean lifetime $<\tau>$ is calculated as $<\tau> = \Sigma\ \alpha_i\tau_i$

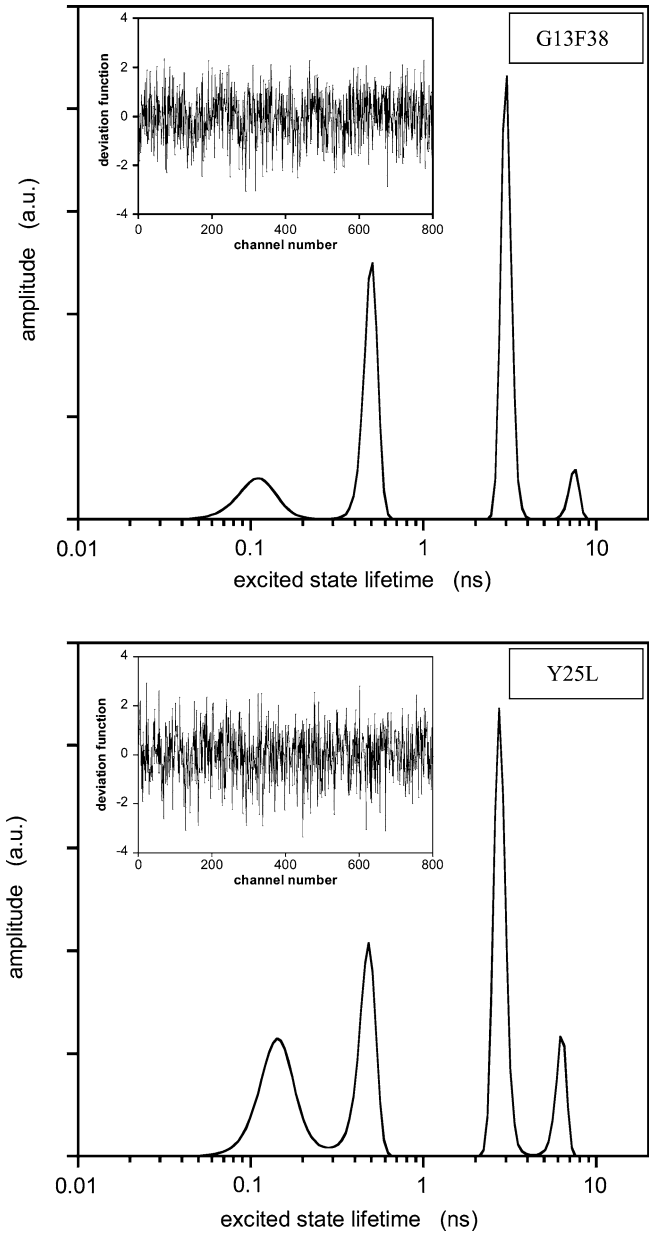


**Fig. 4** MEM recovered lifetime distributions of G13-F38 and Y25L in DPC micelles. G13-F38 (upper panel) and Y25L (lower panel) were added at a final concentration of 5 μM to 4 mM DPC in 10 mM potassium phosphate buffer pH 7.5, at 20°C. $\lambda_{ex}$ was set at 292 nm and $\lambda_{em}$ at 334 nm, excitation and emission bandwidths: 4 and 8 nm, respectively. Parameters of the distribution are given in Table 1. Data are representative of two sets of experiments. Insets: deviation function of the fits

relation time ($\theta$) values, with $\theta_2$ ~2 ns, indicating that the fragments were soluble in aqueous medium as small peptide oligomers, if not monomers. The observed heterogeneity of decay may also indicate segmental motion of the fragments.

In detergent micelles, a single component was obtained, the rotational correlation time ($\theta$) value being in the range expected for a whole detergent micelle (values of 21 ns and 7.5 ns were calculated for DM and DPC micelles, respectively, without taking into account hydration, see Materials and methods. They respectively correspond to micelle molecular weight of~65,000 and 20,000). The lack of shorter $\theta$ values suggests that exchanges between Trp rotamers were slow and therefore, undetectable and that the peptide rotated slowly within the micelle, over the time scale of fluorescence, with Trp rotation reflecting the rotation of the whole peptide-detergent complex. Our results also suggest that the insertion of the peptide into micelles has no major effect on their sizes. In all cases, anisotropy at time zero (the mean value for the fragments in detergent was $0.145 \pm 0.014$) was similar to the fundamental anisotropy of indole at the same $\lambda_{ex}$ (0.150), also ruling out the possibility of motions too rapid for analysis (below ~100 ps).

**Table 2** Parameters of the anisotropy decays of G13-F38 and Y25L in DPC or DM micelles, or buffer

| Peptide | Solvent | $\beta_1$ | $\beta_2$ | $\theta_1$ (ns) | $\theta_2$ (ns) | $A_{t=0}$ | $\chi^2$ |
|---|---|---|---|---|---|---|---|
| G13-F38 | DPC | | 0.154 | | 11.3 | 0.154 | 0.97 |
| Y25L | | | 0.151 | | 11.8 | 0.151 | 1.01 |
| G13-F38 | DM | | 0.124 | | 13.8 | 0.124 | 1.06 |
| Y25L | | | 0.151 | | 22.7 | 0.151 | 0.98 |
| G13-F38 | Buffer | 0.083 | 0.080 | 0.45 | 2.38 | 0.163 | 1.02 |
| Y25L | | 0.002 | 0.091 | 0.36 | 1.51 | 0.093 | 0.99 |

Conditions were as in Table 1. $\beta_i$ is the area and $\theta_i$ the barycenter of each peak of the rotational correlation time distribution. $A_{t=0}$ is the anisotropy value at time zero, with $A_{t=0} = \sum \beta_i$

## Quenching of G13-F38 and Y25L in mixed micelles of brominated and non-brominated detergent

We carried out Trp quenching experiments with G13-F38 and Y25L, in the presence of mixed micelles consisting of dodecylmaltoside and a brominated analog (BrDM or BrUM) (Fig. 5). They were interpreted in terms of accessibility of Trp to the two bromine atoms located at various positions in the acyl chain of the detergent (close to the middle, on C7-C8 for BrDM and at the end, on C10-C11 for BrUM). The depth at which Trp residues were inserted within the micelles was estimated by comparison with calibration curves generated with a set of model peptides (de Foresta et al. 2002).

The quenching plots exhibited curved shapes, to which we fitted the function $F/F_0 = (1\text{-}F_{min}/F_0)(1\text{-}X)^n + F_{min}/F_0$ (see Materials and methods). In all cases, the residual fluorescence observed in pure brominated detergent micelles (i.e. at $X = 1$) was very weak ($F_{min}/F_0 < 10\%$) indicating that almost all peptides were bound to micelles with Trp in the close vicinity of at least some bromine atoms. If BrUM was used as the quencher, the curves for G13-F38 and Y25L merged, yielding very similar n values (4 and 3.9, respectively), with $n$ reflecting the number of detergent chains able to bring their bromine atoms close enough (for quenching) to the Trp residue at the same time. If BrDM was used as the quencher, the curves for G13-F38 and Y25L were

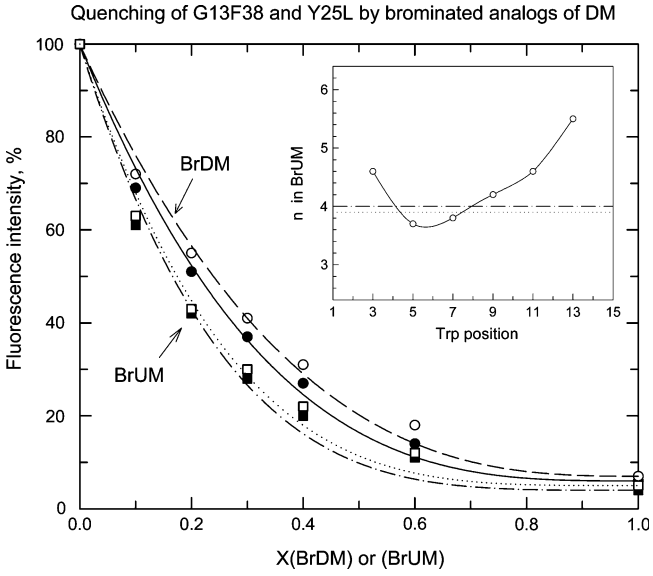


**Fig. 5** Quenching of G13-F38 and Y25L fluorescence in mixed micelles of BrDM/DM (circles) or BrUM/DM (squares). G13-F38 (closed symbols) or Y25L (open symbols) (5 μM) was added to 10 mM potassium phosphate buffer pH 7.5 supplemented with a mixture of BrDM and DM, or BrUM and DM, at a final total detergent concentration of 4 mM, at 20°C. The resulting fluorescence intensity was recorded for 150 s or 200 s to allow equilibration and the final fluorescence intensity was corrected for blank value (detergents in buffer) and plotted as a function of the molar fraction of brominated detergent X, defined as X = [BrDM]/([BrDM] + [DM]) or [BrUM]/([BrUM] + [DM]). X was varied between 0 (pure DM micelles) and 1 (pure BrDM or BrUM micelles). $\lambda_{ex}$ was set at 280 nm and $\lambda_{em}$ at 334 nm, with slit widths of 1.25 mm for both excitation and emission. Data points are the mean of duplicate measurements. The function $F/F_0 = (1-F_{min}/F_0)(1-X)^n + F_{min}/F_0$ was fitted to the data (see Materials and Methods). The inset reports the calibration curve of n for BrUM obtained with six model peptides, where n is plotted as a function of Trp position in the peptide (de Foresta et al. 2002). The two horizontal lines represent the n values, with BrUM, obtained in the experiments reported in this paper (same lines as in the main Figure)

both located higher up the *y* axis than those obtained with BrUM (this was also true for all model peptides previously studied) and the *n* values obtained were lower and differed slightly (3.2 and 2.8, respectively).

In both cases, these *n* values fall in the range of values obtained for model peptides (see Fig. 5 inset for BrUM). The intersections of the two horizontal lines (n values for G13-F38 and Y25L) with the calibration curve indicated that W28 was located close to Trp in the P5 and/or P7 model peptides. The results obtained with BrDM are also consistent with such a position but the calibration curve was more complex in this case (de Foresta et al. 2002).

## Quenching of G13-F38 and Y25L by acrylamide

Acrylamide is a neutral, water-soluble, highly efficient quenching probe, and was used to test the accessibility of Trp to the aqueous phase. It was used for both peptide-DM and peptide-DPC complexes.

Stern-Volmer plots of quenching (Fig. 6) clearly showed that the Trp residues of G13-F38 and Y25L were only poorly accessible when these fragments were embedded in DM or DPC micelles. This is demonstrated by the lower $K_{sv}$ values for the corresponding Stern–Volmer plots than for the plots obtained for NATA in buffer taken as the reference for fully accessible Trp. The slopes obtained were much higher for peptides in buffer alone than in detergent, providing additional evidence of the solubility in water of these peptides.

Quenching parameters are reported in Table 3, including the bimolecular quenching constant $k_q$, which takes into account the effects of various lifetimes. Both peptides displayed similar levels of Trp accessibility in each medium (with only a slight difference in DPC), with accessibility depending on the medium. In DM, the accessibility of 18% obtained is very similar to that previously obtained for TOE, a hydrophobic model of Trp, in the same medium (22%). In contrast, the accessibility of W28 in DPC (26–33%) was much lower than that of TOE in DPC (72%; Tortech et al. 2001). The presence of the peptide interfacial loop may contribute to this difference. In buffer, W28 was almost completely accessible (87%) (±1%). The similar values obtained for these peptides in DM and DPC suggest that they are anchored within these different micelles in a very similar way, significantly embedded in the micelle but not in the deeper core (accessibility of only 5–15%

**Table 3** Parameters of PMP1 fragments fluorescence quenching by acrylamide

| Fluorophore | Medium | $<\tau>$ (ns) | $K_{sv}$ ($M^{-1}$) | $k_q$ ($M^{-1}$ $s^{-1}$) | Percentage of reference (%) |
|---|---|---|---|---|---|
| NATA | Buffer | 3.0 | 18.9 | $6.30\times10^9$ | 100 |
| G13-F38 | DPC | 1.91 | 3.18 | $1.66\times10^9$ | 26 |
| Y25L | | 1.72 | 3.57 | $2.07\times10^9$ | 33 |
| G13-F38 | DM | 2.26 | 2.51 | $1.11\times10^9$ | 18 |
| Y25L | | 2.31 | 2.66 | $1.15\times10^9$ | 18 |
| G13-F38 | Buffer | 2.34 | 12.7 | $5.43\times10^9$ | 86 |
| Y25L | | 2.38 | 13.2 | $5.54\times10^9$ | 88 |

The mean lifetime $<\tau>$ is calculated as $<\tau> = \Sigma\ \alpha_i\tau_i$. $<\tau>$ for the fragments are from Table 1. $<\tau>$ for NATA was as reported by Rouvière et al. (Rouvière et al. 1997). $K_{sv}$was taken from Fig. 6 (Stern–Volmer equation: $F_0/F = 1 + K_{sv}[Q]$). The bimolecular quenching constant was calculated as $k_q = K_{sv}/<\tau>$

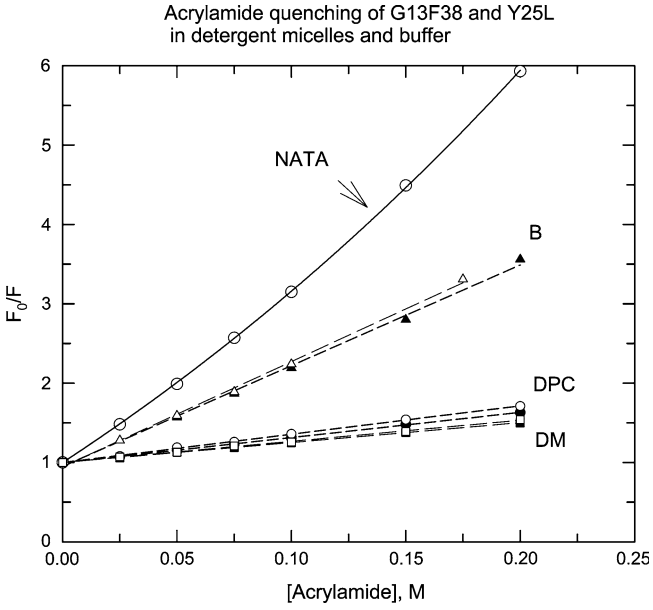


**Fig. 6** Stern-Volmer plots of acrylamide quenching of G13-F38 and Y25L in DPC and DM micelles and buffer, and of NATA in buffer (open circles). G13-F38 (closed symbols) or Y25L (open symbols) (8 μM) was added to 10 mM phosphate buffer pH 7.5, at 20°C, alone (triangles) or together with 4 mM DPC (circles) or DM (squares). Aliquots of acrylamide were then added sequentially, at 100 s intervals. Fluorescence intensity was recorded continuously with $\lambda_{ex}$ set at 295 nm (to minimize inner filter effects due to acrylamide absorption) and $\lambda_{em}$ at 350 nm in buffer or 340 nm (slightly shifted with respect to $\lambda_{max}$ to prevent Raman peak contribution) in the presence of detergent. Slit widths were 1.25 mm for excitation and 2.5 mm for emission. The fluorescence intensities obtained at each acrylamide concentration were corrected for blank values. For reference, a similar experiment (but with $\lambda_{em}$ set at 354 nm) was performed with NATA (5 μM) in buffer. Linear regression was performed for the data obtained for the peptides (dashed lines) whereas a modified Stern-Volmer plot, $F_0/F = (1 + K_{sv}[Q])\exp V[Q]$ was used for NATA (V, sphere of action of static quenching)

were obtained for the model peptides P11-P13 in DPC, unpublished data).

## Discussion

This paper focused on various factors governing insertion into membrane of a small regulatory protein PMP1. For this purpose, we investigated the fluorescence properties and location of the single Trp (W28) of PMP1 in various synthetic fragments—mainly G13-F38 and its mutated form Y25L—incorporated into micelles of DM or DPC, which were used as membrane mimics.

Based on known membrane protein structures, Trp and Tyr residues seem to be preferentially located at interfacial regions of the membrane (Killian and von Heijne 2000; Ulmschneider and Sansom 2001). This preference has also been demonstrated for isolated Trp analogs, which are preferentially located at the interface, in the vicinity of glycerol groups in phosphatidylcholine membranes (Yau et al. 1998), see also (Persson et al. 1998). In addition to various factors, such as hydrogen bonding and dipolar moment, the flat shape and quadrupolar moment of Trp have also been shown to be important (Yau et al. 1998). If Trp plays specific roles in some membrane proteins, it may also be important in membrane protein folding, stabilizing the anchorage of transmembrane helices (de Planque et al. 2003; Ridder et al. 2000).

We investigated PMP1 anchorage in complexes of fragments with DM or DPC and found that various results supported a location of the W28 indole moiety below but close to the polar headgroups of the detergent, in the presence or absence of Y25. In the conditions used for most of the experiments (5–10 μM peptide and 4 mM detergent), G13-F38 and the mutant form Y25L were completely bound to detergent micelles, as shown by binding curves. This finding is consistent with those for the brominated detergent quenching experiments. The detergent was also present in a large molar excess, minimizing possible peptide–peptide interactions (400–800 moles detergent/mole peptide, i.e., 3–12 detergent micelles per peptide, taking into account detergent cmc and aggregation numbers). The resulting fluorescence signals were stable and the peptide-detergent complexes were similar in size to pure micelles, as shown from anisotropy decay measurements. This finding is consistent with previous NMR results (phosphorus relaxation measurements for DPC), showing that the DPC-(PMP1 fragment) complex was only slightly larger than the DPC micelle (Beswick et al. 1998a). The hydrophobic anchor of G13-F38 fragments is essential for complex formation as the shorter fragment, Y25-F38, interacts only weakly with DPC (see the binding curve), and does not interact in a detectable manner with DM.

We determined the location of W28 from emission spectra, characterized by $\lambda_{max}$ values, combined with fluorescence quenching efficiencies with various compounds. $\lambda_{max}$ has long been known to reflect the polarity of the Trp microenvironment and was recently shown to be predictable from the local electric field, due to a so-called internal Stark effect (Vivian and Callis 2001). For micelles, this effect is partly related to water penetration within the micelle. The $\lambda_{max}$ for G13-F38 fragments (334 nm in DM and DPC) is 15 nm lower than that observed for G13-F38 in aqueous solution (349 nm) but significantly higher than that of model peptides with Trp deeply embedded in the micelle ($\lambda_{max}$ = 320 to 313 nm for P9 to P13).

Accessibility of W28 to acrylamide was low in both detergents. In particular, it was much lower in DPC than that of TOE, a hydrophobic model for Trp. TOE is much less firmly anchored in the micelle than G13-F38 fragments, displays rapid local rotational motion (Tortech et al. 2001) and its position with respect to the interface may fluctuate.

We also describe, for the first time, the use of two brominated analogs of DM—BrDM and BrUM—as quenchers, with our interpretation based on comparison

with calibration data recently obtained with six model peptides (de Foresta et al. 2002). Our initial studies of the quenching of transmembrane fragments of a membrane transporter (sarcoplasmic reticulum (SR) $Ca^{2+}$-ATPase) solubilized in DM micelles showed that such calibration was essential for correct interpretation of the data (Soulié et al. 1998). The results presented here indicate that W28 is located in a position similar to that of Trp in the P5-P7 peptides. BrUM (bromines in C10-C11 positions) appeared to be more suitable than BrDM for predicting Trp location because the calibration curve of the parameter "*n*" was simpler with BrUM, and relative variations in n were greater. Plots of the radial density of individual carbon atoms obtained from molecular dynamics simulations of DPC or SDS micelles has shown that the tail atoms of the hydrophobic chain have a broad radial distribution within the micelle (MacKerell 1995; Tieleman et al. 2000): this may account for the larger values of *n* obtained for quenching by BrUM than for quenching by BrDM (with the exception of TOE). In addition, as the hydrocarbon chain of BrUM is one carbon shorter than that of BrDM, the density of bromines within the BrUM micelle may be slightly higher, and the slightly smaller micelles obtained may also contribute to this effect.

Such an intermediate location of Trp is consistent with the $\lambda_{max}$ values, that exclude deeper location, and with the low accessibility to acrylamide, that exclude interfacial location. It is also compatible with the $<\tau>$ values. Also taking into account the structure of the (α-helical) model peptides-detergent complexes (see scheme 1 in de Foresta et al. 2002), this position would be below but close to the polar headgroup region.

This position of W28 is consistent with the NMR results obtained in DPC. We additionally showed here that this residue was located in the same position in both DM and DPC. The strict conservation of this position probably also results from the immobilization of the peptides with respect to the micelles, as shown by anisotropy decay measurements. The well-defined characteristics of W28 are consistent with its functional role: the W28L mutation causes a loss of POPS binding specificity and concomitant structural changes thoroughly analyzed (Mousson et al. 2001a, 2002), such as loss of the Q32-W28 H-bond and extension of the helix to L35. Among these various changes, an indirect effect via changes for Q32, which was proposed to interact with the serine group of POPS, may be of particular importance. Similarly W23 from the C-terminal part of sarcolipin (sequence -$WLLVRSYQY_{31}$) was also shown to be embedded in the hydrophobic part of the membrane, from both emission spectra and quenching curves by brominated phospholipids (Smith et al. 2002).

The peptides G13-F38 and Y25L display lifetime heterogeneity in DM, DPC and buffer. Lifetime heterogeneity in proteins has long been thought to be correlated with Trp rotamers, based on the differences in the local environments of these rotamers, in particular the distances to various quenchers (Chen and Barkley 1998). Eight amino acids have been identified as quenchers (in decreasing order of efficiency): tyrosine, cysteine and positively charged histidine (strong quenchers), neutral glutamic acid and aspartic acid (moderate quenchers) and lysine, glutamine, asparagine and neutral histidine (weak quenchers). They act by excited-state proton transfer or electron transfer. More recently, the major role in Trp quenching played by the backbone peptide bond (by excited state electron transfer) has been assessed, and a correlation has been found between single Trp rotamers and lifetime values (Ababou and Bombarda 2001; Adams et al. 2002; Liu et al. 2002; Pan and Barkley 2004; Sillen et al. 2000). However, Trp is preferentially present as six rotamers: three $\chi_1$ rotamers around the $C_\alpha$-$C_\beta$ bond ($\chi_1 = \pm 60°, 180°$) combined with two $\chi_2$ rotamers around the $C_\beta$-$C_\gamma$ bond ($\chi_2 = \pm 90°$). Assignment is generally not straightforward. For small peptides, $\chi_1$ rotamers are thought to be the main source of lifetime heterogeneity. The lifetime distribution presented here differs significantly from that obtained with the polyLeu model peptides: for these peptides, the two longest components (centered at ~2.3 and 5 ns) accounted for the main part of the distribution whereas for PMP1 peptides, the two intermediate components (~0.5 and 3 ns) were those mainly populated. These differences are related to the specific constrained structure of PMP1 (see Results). Using the assignment of lifetimes to particular rotamers in fluorescent cyclic hexapeptides (Pan and Barkley 2004), we suggest that the $\tau_2$ (0.5 ns) and $\tau_3$ (3 ns) components correspond to the $\chi_1 = 60°$ and $\chi_1 = 180°$ rotamers of W28, respectively. However, the data should be interpreted with caution due to the possible influence of $\chi_2$ rotamers and the presence of the shorter lived component. NMR data have also shown that W28 presents an uneven distribution of rotamers in DPC, with the $\chi_1 = 180°$ rotamer favored. Recent analyses have shown that membrane environment alters the rotamer preferences asymmetrically, the frequencies of rotamers favoring snorkeling for Trp, i.e., a tendency for its polar N atom to extend out of the membrane (here micelle), being increased. On the C-terminal halves of helices, this is the case for some $\chi_1 = 180°$ rotamers which are predominant (Chamberlain and Bowie 2004). For PMP1, a stacking effect between the side chains of W28 and Q32 has also been demonstrated (Beswick et al. 1998b; Mousson et al. 2001a).

The G13-F38 fragments were found to be immobilized in the micelles, the single correlation time obtained in each detergent (~12 and 18 ns as an average in DPC and DM, respectively) reflecting the rotation of the whole micelle. This is a particularly striking result because no such immobilization was observed for any of the model peptides in these detergents. In DM, for instance, a shorter component ($\theta_1$ ~3 ns) was present in a significant proportion (~15–30%). This is likely due to the specific folding of the C-terminal domain of PMP1 partly stabilized by an H-bond between W28 and Q32. Interestingly, such immobilization was recently reported for the transmembrane domain of phospholamban in

DPC, based on NMR spectroscopy (Metcalfe et al. 2004). The structural and dynamics homologies between these two peptides suggests that these shared characteristic may be of biological significance in their target recognition.

## Conclusion

We compared the fluorescence of the G13-F38 fragment of PMP1 and its mutated form, Y25L in membrane mimetic systems. The C-terminal domain conformation of this lipid-binding protein has been shown to be important for its function and to be regulated by a complex network of interactions, from studies with fragments of various lengths and various mutants (Mousson et al. 2001a). We showed in this study that the characteristics of Trp, shown to be located below but close to the polar headgroups, remain remarkably constant in DM and DPC, in the presence or absence of Y25. The quenching method applied—with the use of brominated detergents (de Foresta et al. 1996) and calibration data (de Foresta et al. 2002)—gave results consistent with previous NMR experiments in DPC, which further validates this approach. We also clearly demonstrated that the DPC polar headgroup favors the structuring of amphipathic peptides, such as Y25-F38, to a greater extent than DM. Finally, we have initiated studies of the full-length PMP1 protein, which has been synthesized and shown to form complexes with both DM and DPC.

**Acknowledgements** We thank the technical staff of the Laboratoire pour l'Utilisation du Rayonnement Electromagnétique (LURE) for running the synchrotron ring during the beam sessions.

## References

Ababou A, Bombarda E (2001) On the involvement of electron transfer reactions in the fluorescence decay kinetics heterogeneity of proteins. Protein Sci 10:2102–2113

Adams PD, Chen Y, Ma K, Zagorski MG, Sönnichsen FD, McLaughlin ML, Barkley MD (2002) Intramolecular quenching of tryptophan fluorescence by the peptide bond in cyclic hexapeptides. J Am Chem Soc 124:9278–9286

Asahi M, Kimura Y, Kurzydlowski K, Tada M, MacLennan DH (1999) Transmembrane helix M6 in sarco(endo)plasmic reticulum $Ca^{2+}$-ATPase forms a functional interaction site with phospholamban. Evidence for physical interactions at other sites. J Biol Chem 274:32855–32862

Asahi M, Sugita Y, Kurzydlowski K, De Leon S, Tada M, Toyoshima C, MacLennan DH (2003) Sarcolipin regulates sarco(endo)plasmic reticulum $Ca^{2+}$-ATPase (SERCA) by binding to transmembrane helices alone or in association with phospholamban. Proc Natl Acad Sci USA 100:5040–5045

Beswick V, Guerois R, Cordier-Ochsenbein F, Coïc YM, Huynh-Dinh T, Tostain J, Noël JP, Sanson A, Neumann JM (1998a) Dodecylphosphocholine micelles as a membrane-like environment: new results from NMR relaxation and paramagnetic relaxation enhancement analysis. Eur Biophys J 28:48–58

Beswick V, Roux M, Navarre C, Coïc YM, Huynh-Dinh T, Goffeau A, Sanson A, Neumann JM (1998b) $^{1}$H- and $^{2}$H-NMR studies of a fragment of PMP1, a regulatory subunit associated with the yeast plasma membrane $H^{+}$-ATPase. Conformational properties and lipid–peptide interactions. Biochimie 80:451–459

Bouhss A, Vincent M, Munier H, Gilles A-M, Takahashi M, Bârzu O, Danchin A, Gallay J (1996) Conformational transitions within the calmodulin–binding site of *Bordetella pertussis* adenylate cyclase studied by time-resolved fluorescence of Trp242 and circular dichroism. Eur J Biochem 237:619–628

Brochon JC (1994) Maximum entropy method of data analysis in time-resolved spectroscopy. Methods Enzymol 240:262–311

Brown LR, Bösch C, Wüthrich K (1981) Location and orientation relative to the micelle surface for glucagon in mixed micelles with dodecylphosphocholine: EPR and NMR studies. Biochim Biophys Acta 642:296–312

Chamberlain AK, Bowie JU (2004) Analysis of side-chain rotamers in transmembrane proteins. Biophys J 87:3460–3469

Chan WC, White PD (2000) Fmoc solid phase peptide synthesis. A practical approach. Oxford University Press, New York

Chen Y, Barkley MD (1998) Toward understanding tryptophan fluorescence in proteins. Biochemistry 37:9976–9982

Dupuy C, Auvray X, Petipas C, Rico-Lattes I, Lattes A (1997) Anomeric effects on the structure of micelles of alkyl maltosides in water. Langmuir 13:3965–3967

East JM, Lee AG (1982) Lipid selectivity of the calcium and magnesium ion dependent adenosinetriphosphatase, studied with fluorescence quenching by a brominated phospholipid. Biochemistry 21:4144–4151

Eftink MR (1991) Fluorescence techniques for studying protein structure. Methods Biochem Anal 35:127–205

Fernández C, Wüthrich K (2003) NMR solution structure determination of membrane proteins reconstituted in detergent micelles. FEBS Lett 555:144–150

de Foresta B, Legros N, Plusquellec D, le Maire M, Champeil P (1996) Brominated detergents as tools to study protein-detergent interactions. Eur J Biochem 241:343–354

de Foresta B, Gallay J, Sopkova J, Champeil P, Vincent M (1999) Tryptophan octyl ester in detergent micelles of dodecylmaltoside: fluorescence properties and quenching by brominated detergent analogs. Biophys J 77:3071–3084

de Foresta B, Tortech L, Vincent M, Gallay J (2002) Location and dynamics of tryptophan in transmembrane alpha-helix peptides: a fluorescence and circular dichroism study. Eur Biophys J 31:185–197

Jones DH, Golding MC, Barr KJ, Fong GH, Kidder GM (2001) The mouse $Na^{+}$ -$K^{+}$-ATPase $\gamma$-subunit gene (*Fxyd2*) encodes three developmentally regulated transcripts. Physiol Genomics 6:129–135

Killian JA, von Heijne G (2000) How proteins adapt to a membrane-water interface. Trends Biochem Sci 25:429–434

Lakowicz JR (1999) Principles of fluorescence spectroscopy. Kluwer, New York

Lauterwein J, Bösch C, Brown LR, Wüthrich K (1979) Physicochemical studies of the protein–lipid interactions in melittin-containing micelles. Biochim Biophys Acta 556:244–264

Le Maire M, Champeil P, Møller JV (2000) Interaction of membrane proteins and lipids with solubilizing detergents. Biochim Biophys Acta 1508:86–111

Liu B, Thalji RK, Adams PD, Fronczek FR, McLaughlin ML, Barkley MD (2002) Fluorescence of *cis*-1-amino-2-(3-indolyl)cyclohexane-1-carboxylic acid: a single tryptophan $\chi_1$ rotamer model. J Am Chem Soc 124:13329–13338

Livesey AK, Brochon JC (1987) Analyzing the distribution of decay constants in pulse-fluorimetry using the maximum entropy method. Biophys J 52:693–706

London E, Feigenson GW (1981) Fluorescence quenching in model membranes. 1 Characterization of quenching caused by a spin-labeled phospholipid. Biochemistry 20:1932–1938

MacKerell AD Jr (1995) Molecular dynamics simulation analysis of a sodium dodecyl sulfate micelle in aqueous solution: decreased fluidity of the micelle hydrocarbon interior. J Phys Chem 99:1846–1855

Mascioni A, Karim C, Barany G, Thomas DD, Veglia G (2002) Structure and orientation of sarcolipin in lipid environments. Biochemistry 41:475–482

Metcalfe EE, Zamoon J, Thomas DD, Veglia G (2004) $^{1}$ H/$^{15}$ N heteronuclear NMR spectroscopy shows four dynamic domains for phospholamban reconstituted in dodecylphosphocholine micelles. Biophys J 87:1205–1214

Møller JV, le Maire M (1993) Detergent binding as a measure of hydrophobic surface area of integral membrane proteins. J Biol Chem 268:18659–18672

Møller JV, le Maire M, Andersen JP (1986) Uses of non-ionic and bile salt detergents in the study of membrane proteins. In: Watts et de Pont (eds) "Progress in Protein-Lipid Interactions" vol 2. Elsevier Science Publishers BV (Biomedical division), pp 147–196

Mousson F, Beswick V, Coïc YM, Baleux F, Huynh-Dinh T, Sanson A, Neumann JM (2001a) Concerted influence of key amino acids on the lipid binding properties of a single-spanning membrane protein: NMR and mutational analysis. Biochemistry 40:9993–10000

Mousson F, Beswick V, Coïc YM, Huynh-Dinh T, Sanson A, Neumann JM (2001b) Investigating the conformational coupling between the transmembrane and cytoplasmic domains of a single-spanning membrane protein A $^{1}$ H-NMR study. FEBS Lett 505:431–435

Mousson F, Coïc YM, Baleux F, Beswick V, Sanson A, Neumann JM (2002) Deciphering the role of individual acyl chains in the interaction network between phosphatidylserines and a single-spanning membrane protein. Biochemistry 41:13611–13616

Navarre C, Ghislain M, Leterme S, Ferroud C, Dufour JP, Goffeau A (1992) Purification and complete sequence of a small proteolipid associated with the plasma membrane $H^+$-ATPase of *Saccharomyces cerevisiae*. J Biol Chem 267:6425–6428

Navarre C, Catty P, Leterme S, Dietrich F, Goffeau A (1994) Two distinct genes encode small isoproteolipids affecting plasma membrane $H^+$-ATPase activity of *Saccharomyces cerevisiae*. J Biol Chem 269:21262–21268

Pan CP, Barkley MD (2004) Conformational effects on tryptophan fluorescence in cyclic hexapeptides. Biophys J 86:3828–3835

Persson S, Killian JA, Lindblom G (1998) Molecular ordering of interfacially localized tryptophan analogs in ester- and ether-lipid bilayers studied by $^{2}$ H-NMR. Biophys J 75:1365–1371

Peterson GL, Rosenbaum LC, Schimerlik MI (1988) Solubilization and hydrodynamic properties of pig atrial muscarinic acetylcholine receptor in dodecyl $\beta$-D-maltoside. Biochem J 255:553–560

de Planque MR, Bonev BB, Demmers JA, Greathouse DV, Koeppe II RE, Separovic F, Watts A, Killian JA (2003) Interfacial anchor properties of tryptophan residues in transmembrane peptides can dominate over hydrophobic matching effects in peptide–lipid interactions. Biochemistry 42:5341–5348

Reshetnyak YK, Koshevnik Y, Burstein EA (2001) Decomposition of protein tryptophan fluorescence spectra into log-normal components III Correlation between fluorescence and microenvironment parameters of individual tryptophan residues. Biophys J 81:1735–1758

Ridder AN, Morein S, Stam JG, Kuhn A, de Kruijff B, Killian JA (2000) Analysis of the role of interfacial tryptophan residues in controlling the topology of membrane proteins. Biochemistry 39:6521–6528

Ross JB, Wyssbrod HR, Porter RA, Schwartz GP, Michaels CA, Laws WR (1992) Correlation of tryptophan fluorescence intensity decay parameters with $^{1}$ H NMR-determined rotamer conformations: [tryptophan$^{2}$ ]oxytocin. Biochemistry 31:1585–1594

Rouvière N, Vincent M, Craescu CT, Gallay J (1997) Immunosuppressor binding to the immunophilin FKBP59 affects the local structural dynamics of a surface $\beta$-strand: time-resolved fluorescence study. Biochemistry 36:7339–7352

Roux M, Beswick V, Coïc YM, Huynh-Dinh T, Sanson A, Neumann JM (2000) PMP1 18–38, a yeast plasma membrane protein fragment, binds phosphatidylserine from bilayer mixtures with phosphatidylcholine: a $^{2}$ H-NMR study. Biophys J 79:2624–2631

Sillen A, Díaz JF, Engelborghs Y (2000) A step toward the prediction of the fluorescence lifetimes of tryptophan residues in proteins based on structural and spectral data. Protein Sci 9:158–169

Smith W, Broadbridge R, East JM, Lee AG (2002) Sarcolipin uncouples hydrolysis of ATP from accumulation of $Ca^{2+}$ by the $Ca^{2+}$-ATPase of skeletal muscle sarcoplasmic reticulum. Biochem J 361:277–286

Soulié S, de Foresta B, Møller JV, Bloomberg GB, Groves JD, le Maire M (1998) Spectroscopic studies of the interaction of $Ca^{2+}$-ATPase-peptides with dodecyl maltoside and its brominated analog. Eur J Biochem 257:216–227

Szabo AG, Rayner DM (1980) Fluorescence decay of Trp conformers in aqueous solution. J Am Chem Soc 102:554–563

Tieleman DP, van der Spoel D, Berendsen HJC (2000) Molecular dynamics simulations of dodecylphosphocholine micelles at three different aggregate sizes: micellar structure and chain relaxation. J Phys Chem B 104:6380–6388

Tortech L, Jaxel C, Vincent M, Gallay J, de Foresta B (2001) The polar headgroup of the detergent governs the accessibility to water of tryptophan octyl ester in host micelles. Biochim Biophys Acta 1514:76–86

Ulmschneider MB, Sansom MSP (2001) Amino acid distributions in integral membrane protein structures. Biochimica Biophysica Acta (BBA) Biomembranes 1512:1–14

Vivian JT, Callis PR (2001) Mechanisms of tryptophan fluorescence shifts in proteins. Biophys J 80:2093–2109

Willis KJ, Neugebauer W, Sikorska M, Szabo AG (1994) Probing $\alpha$-helical secondary structure at a specific site in model peptides via restriction of tryptophan side-chain rotamer conformation. Biophys J 66:1623–1630

Yau WM, Wimley WC, Gawrisch K, White SH (1998) The preference of tryptophan for membrane interfaces. Biochemistry 37:14713–14718

Zamoon J, Mascioni A, Thomas DD, Veglia G (2003) NMR solution structure and topological orientation of monomeric phospholamban in dodecylphosphocholine micelles. Biophys J 85:2589–2598